Why have not the hairs on the feet of gecko been smaller?

Yewang Su, Shijie He, Keh-Chih Hwang, and Baohua Ji

Citation: Appl. Phys. Lett. **101**, 173106 (2012); doi: 10.1063/1.4762822
View online: http://dx.doi.org/10.1063/1.4762822
View Table of Contents: http://apl.aip.org/resource/1/APPLAB/v101/i17
Published by the American Institute of Physics.

APPLIED PHYSICS LETTERS **101**, 173106 (2012)

Why have not the hairs on the feet of gecko been smaller?

Yewang Su,[1,2,a)] Shijie He,[3] Keh-Chih Hwang,[1] and Baohua Ji[3,a)]
[1]*AML, Department of Engineering Mechanics, Tsinghua University, Beijing 100084, People's Republic of China*
[2]*Department of Civil and Environmental Engineering and Department of Mechanical Engineering, Northwestern University, Evanston, Illinois 60208, USA*
[3]*Biomechanics and Biomaterials Laboratory, Department of Applied Mechanics, School of Aerospace Engineering, Beijing Institute of Technology, Beijing 100081, People's Republic of China*

(Received 3 August 2012; accepted 8 October 2012; published online 23 October 2012)

The nanometer size of the tiny hair is the key to the secret of strong stickiness of gecko's feet, by which the hair can achieve the maximum adhesion strength that is insensitive to the interfacial flaws with substrate surface. But the question why the hairs have not been smaller is not answered yet. In this study, we derived a geometric parameter of the surface structures considering lateral interaction among hairs, which gives a critical size below which these hairs will bunch together and cause failure of the adhesion, suggesting a lower limit of the dimension of hairs on gecko's feet. © *2012 American Institute of Physics*. [http://dx.doi.org/10.1063/1.4762822]

Hair-like surface structures are widely adopted in the surfaces of animals and insects for dry and wet adhesion.[1] These "hairy" biological surfaces consist of finely structured protruding hairs with size ranging from a few hundred nanometers to a few micrometers, depending on animal species. Moreover, the density of hairs increases with the body weight of the animal, and gecko has the highest density among all animal species that have been studied (Fig. 1(a)).[2–5] Various mechanical models have been developed to model the fiber-array structures,[6,7] and significant progress has been made in using the JKR model and fracture model.[4,5] For instance, Arzt *et al.*[5] showed that the hairy surfaces, in which a macroscopic contact area is split into many smaller contact patches, could greatly enhance the adhesive strength. Gao and coworkers[3,4,8] showed that reducing the size of the hairs could increase the adhesion strength and toughness between the hair and substrate, and the adhesion strength became insensitive to the interface flaws when the hair size was reduced to hundreds of nanometers, which suggests an upper limit of the hair size. Yao and Gao[3] further showed that with the hierarchical hair-like surface structures, the gecko's feet could achieve strong and robust adhesion without sensitive to the interfacial flaws at macroscopic scale.

Interestingly, besides the hairy surfaces on gecko's feet for strong adhesion, there are many hairy biological surfaces, however, for superhydrophobic dewetting properties, such as the surfaces of strider's leg and many plant leaves[9–11] (Fig. 1(b)). Similar with the surface of gecko's feet, these biological surfaces also have the nano to micro hierarchical structure, but they are designed to improve the superhydrophobic dewetting properties. It is strikingly interesting that this nano to micro hierarchical surface design can both enhance the gecko-like strong adhesion and the superhydrophobic dewetting properties of the surfaces. Su *et al.*[10–12] did a systematic study of the superhydrophobic biological surfaces, such as the surfaces of water striders' legs and lotus leaves, by addressing several fundamental questions including, why the most elementary surface structure is at the hundreds of nanometers, why the elementary structure cannot be smaller, and what is the role of the surface hierarchy? The first two questions immediately suggested the lower limit and upper limit for the size of the most elementary surface structure. Therefore, for gecko adhesion, a fundamental question is raised: is there also a lower limit for the surface hairy structure? In other words, why have not the hairs on the gecko's feet been smaller?

To answer above questions, let us consider the interaction among multiple hairy fibers. It was shown that the non-contact interaction, such as van der Waals interaction that is negligible at macroscopic scale, would become crucial when the dimension of the system is reduced to nano and micrometer scale.[13] Previous studies showed that in an array of slender hairs planted on a solid surface, the fibers are prone to bundle together under the van der Waals interaction[14,15] (Fig. 1(c)). Hui and coworker derived the anti-bunching condition[15] by considering only two neighboring fibers, suggesting a maximum length of the fiber for the given separation and radius of fibers. However, in previous studies, the effect of the dimension of fibers was not studied. In addition, possible adhesion among multiple fibers was not considered. In this paper, we intend to study the effect of dimension of hairy fibers on their lateral stability by analyzing the anti-bunching conditions of multiple fibers. A scaling law will be derived from the anti-bunching condition, which suggests a critical size below which the hairy fibers are prone to adhere to the neighboring fibers.

Without loss of generality, three patterns of arrangement (triangular ($k=3$), square ($k=4$), and hexagonal ($k=6$))[3] of the fibers with circular cross-section were analyzed as shown in Figs. 2(a1)–2(c1). For the fibers that are bunched up, we denote the number of the fibers in the bundle as n and the number of interfaces among them as m. The values of n and m depend on the pattern and bunching mode (Figs. 2(a2)–2(c2)). The deformations of fibers in the bundle are assumed identical. The strain energy of the bended pillars due to the bending deformation can be calculated by using the beam theory[16,17]

$$U_{k,n} = \frac{6nEIw_{k,n}^2}{L^3}, \tag{1}$$

[a)]Authors to whom correspondence should be addressed. Electronic addresses: suyw05@mails.tsinghua.edu.cn and bhji@bit.edu.cn.

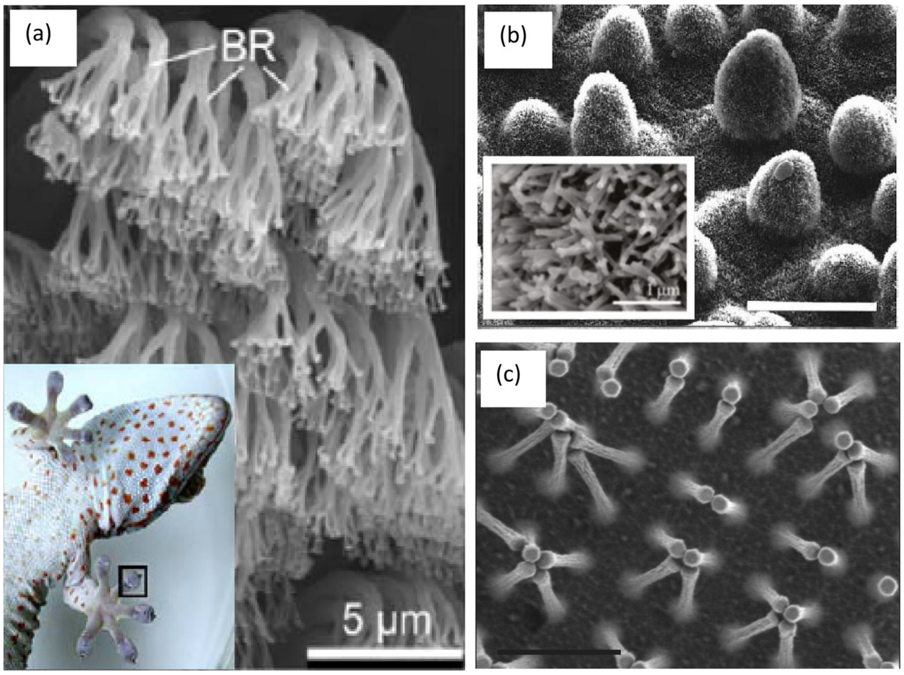

FIG. 1. Typical biological and biomimetic surfaces with hair or pillar like surface structures for various functions. (a) The nano to micro hierarchical hair-like surface structure of geckos' feet for strong adhesion;[8] (b) The nano to micro hierarchical structure of plant leaves for superhydrophobic dewetting properties.[10] (c) The microfabricated polyimide biomimetic hairs bunching together under the van der Waals interaction.[14]

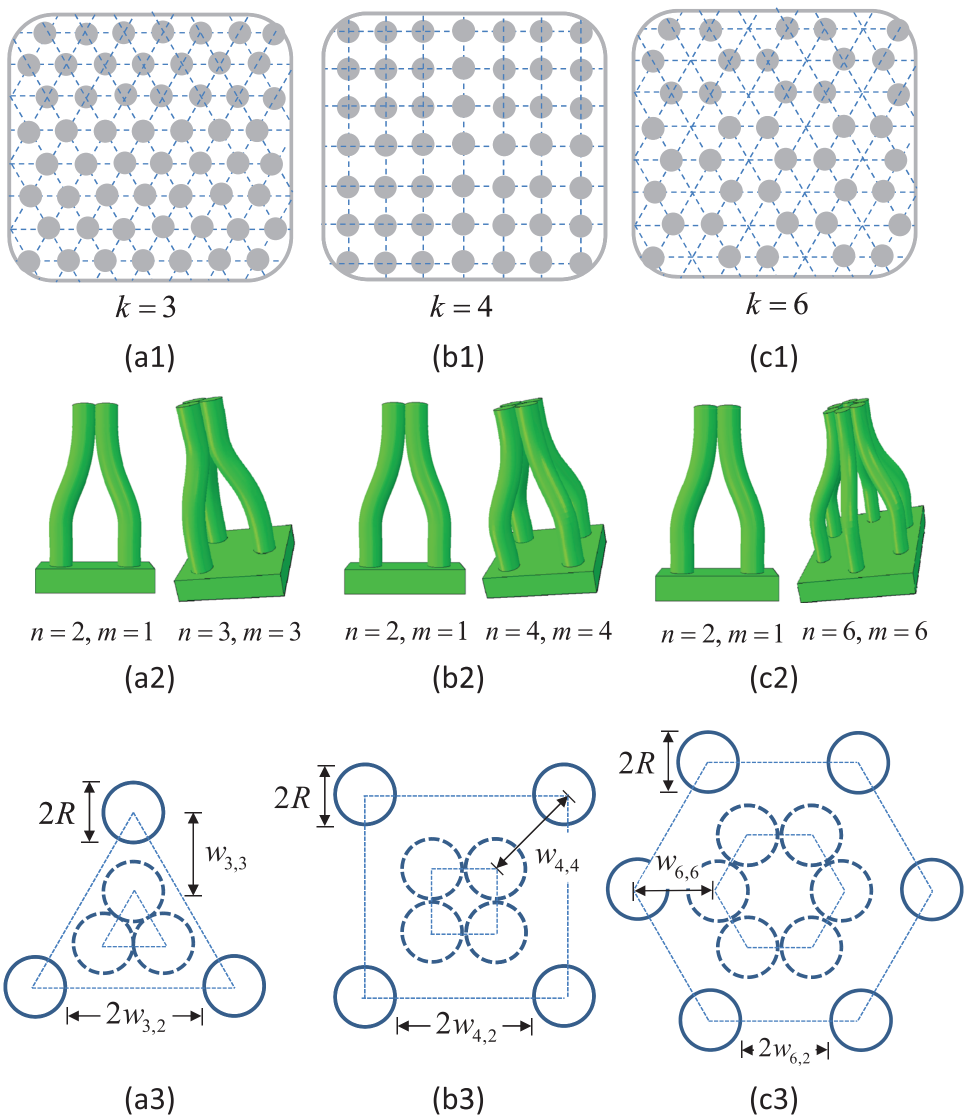

FIG. 2. Schematic illustrations of different surface patterns and bunching modes. (a1)–(c1) for three typical patterns of surface structures: triangular ($k=3$), square ($k=4$), and hexagonal ($k=6$); (a2)–(c2) for illustration of different bunching modes for each surface pattern; (a3)–(c3) for illustration of the lateral displacement of the non-fixed end of fibers for different patterns and bunching modes.

where $E = 1\,\text{GPa}$ is the Young's modulus of the fiber, $I = \pi R^4/4$ is the moment of inertia, R is radius of the fiber, L is the length of the non-contact portion of the fiber, and $w_{k,n}$ is the lateral displacement of the non-fixed end of fibers for the bundle with n fibers in the pattern of type k as shown in Fig. 2(a3)–2(c3). The adhesion work per unit length of the bundle can be obtained according to previous works[15,18]

$$W_{k,n} = 3m\gamma_s \left[\frac{32R^2\gamma_s(1-\nu^2)}{\pi E}\right]^{\frac{1}{3}}, \tag{2}$$

where $\gamma_s = 5mJ/m^2$ is surface energy of fibers, and $\nu = 0.3$ is Poisson's ratio. The length of the non-contact region can be determined by the energy equilibrium at the critical condition of propagation of the non-contact region. Suppose the edges separating the contact and the non-contact regions are advanced by dL. Under the equilibrium conditions, the resulting decrease/increase in strain energy is equal to the energy for separating/combining the surfaces, which is $W_{k,n}dL$. The anti-bunching condition is obtained by equating these two energies, i.e.,

$$-\frac{dU_b}{dL} = W_{k,n}, \tag{3}$$

by which we have

$$g^c_{k,n} = \left[\frac{256m^3(1-\nu^2)}{27n^3\pi^4}\right]^{\frac{1}{4}} \frac{\gamma_s}{E}, \tag{4a}$$

where $g^c_{k,n}$ is the critical value of the geometric parameter group $R_{k,n}\alpha^{2/3}_{k,n}/\rho^3$, and we define

$$g_{k,n} = \frac{R_{k,n}\alpha^{2/3}_{k,n}}{\rho^3}. \tag{4b}$$

If $g_{k,n} < g^c_{k,n}$, the fiber bunching will happen. The critical condition $g_{k,n} = g^c_{k,n}$ for fiber bunching suggests a critical size of fiber as

$$R^c_{k,n} = \frac{g^c_{k,n}\rho^3}{\alpha^{2/3}_{k,n}}, \tag{5}$$

where $\rho = L/R$ is the aspect ratio, and $\alpha_{k,n} = w_{k,n}/R$. The values of $\alpha_{k,n}$ for the three different patterns are listed as below

$$\begin{aligned}
\text{triangular}: \ \alpha_{3,2} &= \sqrt{\frac{\pi}{2\sqrt{3}\varphi}} - 1, \\
\alpha_{3,3} &= \frac{2}{\sqrt{3}}\left(\sqrt{\frac{\pi}{2\sqrt{3}\varphi}} - 1\right), \ 0 < \varphi < \frac{\pi}{2\sqrt{3}} \\
\text{square}: \ \alpha_{4,2} &= \sqrt{\frac{\pi}{4\varphi}} - 1, \\
\alpha_{4,4} &= \sqrt{2}\left(\sqrt{\frac{\pi}{4\varphi}} - 1\right), \ 0 < \varphi < \frac{\pi}{4} \\
\text{hexagonal}: \ \alpha_{6,2} &= \sqrt{\frac{\pi}{3\sqrt{3}\varphi}} - 1, \\
\alpha_{6,6} &= 2\left(\sqrt{\frac{\pi}{3\sqrt{3}\varphi}} - 1\right), \ 0 < \varphi < \frac{\pi}{3\sqrt{3}},
\end{aligned} \tag{6}$$

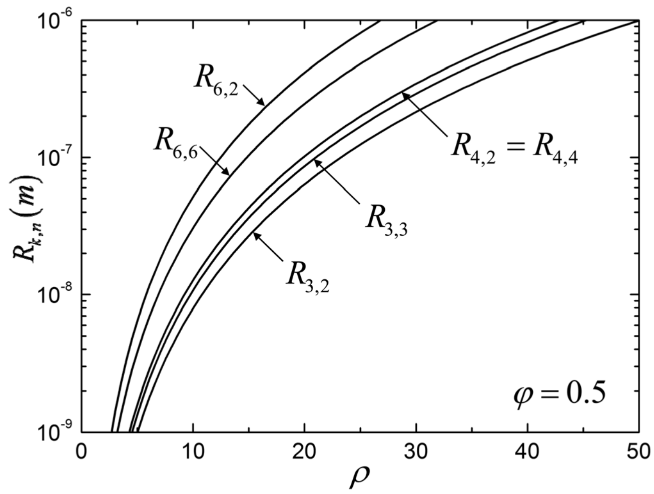

FIG. 3. The relationships between the critical size of fibers and aspect ratio for different surface patterns and bunching modes.

where φ is area fraction, i.e., the ratio between the total area of cross section of the fibers and the total projected area of the patterned surface. In Eq. (6), the first subscript of α indicates the number of fibers in the periodic unit of surface pattern, and the second subscript indicates the number of fibers that are bunched up. For example, $\alpha_{3,2}$ is for the case of the triangular pattern in which two fibers are bunched up, and $\alpha_{3,3}$ is for the case of the triangular pattern in which three fibers are bunched up.

According to Eq. (4a), the critical value of the geometric parameter group $g^c_{k,n}$ is determined by the surface pattern, the material properties and the surface energy.

Equation (5) suggests that once the critical value of the geometric parameter group is given, the critical size of fibers is a function of aspect ratio and area fraction. It defines a lower limit of the dimension of the fibers. That is, the dimension of fibers should be larger than this critical size. Figure 3 shows that the critical size of $R_{k,n}$ increases/decreases with the aspect ratio ρ for different surface patterns and bunching conditions (i.e., bunching of two fibers or bunching of multiple fibers for each pattern). For the hexagonal pattern, the critical size $R^c_{6,2}$ for the case of 2-fiber bunching up is larger than $R^c_{6,6}$ for the case of 6-fiber bunching up, indicating that the 2-fiber bunching are more energy favorable than the 6-fiber bunching in the hexagonal pattern. However, in the triangular pattern the critical size $R^c_{3,2}$ is smaller than $R^c_{3,3}$, which means the 3-fiber bunching is more energy favorable than the 2-fiber bunching. For the square pattern, the critical size $R^c_{4,2} = R^c_{4,4}$, indicating that the 2-fiber bunching and 4-fiber bunching in the square pattern can both happen with the same possibility. Figure 4 shows the relationship between the critical size and the area fraction φ for the 6 different bunching conditions, which suggests that the increase/decrease of area fraction will require the increase/decrease of the critical size.

For example, according to previous works,[2,19] the aspect ratio of the hair of gecko's feet is around 10. If we assume the area fraction is 0.5, the critical size of fibers is in the range of 8–40 nm for different pattern and bunching conditions. The upper limit of the fiber size estimated by Gao and Yao[4] for the robust adhesion is around 100 nm. Therefore,

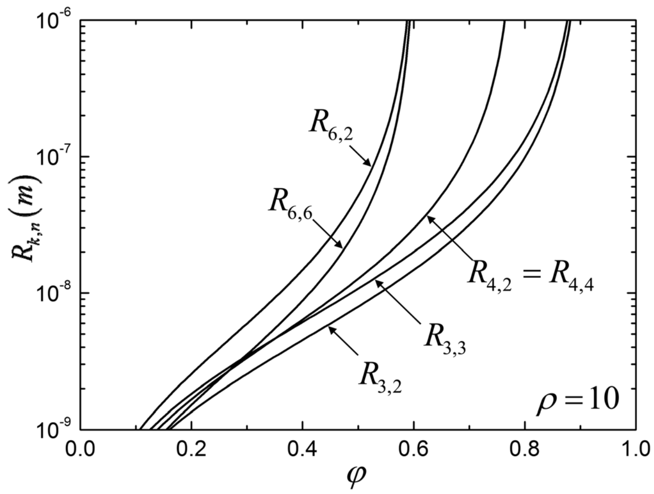

FIG. 4. The relationships between the critical size of fiber and area fraction for different patterns and bunching modes.

these two critical sizes define the range of the selection of dimension of the hairs, which might be the reason why the hairy structures of biological surfaces have not been smaller. If the radius is reduced to $R = 5\,\text{nm}$, the aspect ratio ρ should be reduced to 4–9 for the area fraction $\varphi = 0.5$; or the area fraction φ should be reduced to as small as 0.25–0.4 at the aspect ratio $\rho = 10$. However, the reduction of aspect ratio and area fraction will reduce the robustness and strength of the adhesion, i.e., the lower aspect ratio will cause reduction of energy dissipation of deformation energy in the fibers during their detachment,[8] and the lower area fraction will reduce the apparent adhesion strength $\bar{\sigma} = \varphi\sigma$, where σ is the local adhesion strength between the fiber and substrate. This feature is different from the nanostructure of the bone-like biological materials.[20,21] This result suggests that the size of hairy fiber cannot be unlimited small considering the robustness and strength of the adhesion.

In summary, the anti-bunching behaviors of multiple fibers were analyzed to address the fundamental question why the elementary hairy structure of geckos' feet is at hundreds of nanometers rather than the smaller size. A geometric parameter group consisting of dimension, area fraction, and aspect ratio of hairy fibers was obtained. The critical value of the geometric parameter group presents a scaling law for the dimension of fibers. It suggests a lower limit for the size of fibers below which these fibers will bunch up with neighboring fibers for given aspect ratio, area fraction, and surface patterns. In addition, this geometric parameter group provides a systematic understanding of relationship among these geometric parameters, such as size, area fraction, and aspect ratio, which has not been provided in previous studies. Here, we showed through the anti-bunching analysis these three parameters are closely inter-connected via the geometric parameter group $g^c_{k,n}$ that is determined by the Young's modulus, surface energy, and surface pattern. We should also point it out that in the analysis we implicitly assumed that the fibers have symmetric deformation during the fiber bunching. It can be rigorously derived that the asymmetric deformation will not happen if the size and the mechanical properties of the fibers are all identical, because the total energy of the asymmetric deformation is always higher than that of the symmetric, and the higher the degree of the asymmetry, the more unstable the asymmetric deformation state.[22] This result is consistent with the experimental observation as shown in Fig. 1(c).

Hair-like or pillar-like surface structures are widely used in bio-inspired applications for both adhesion and de-adhesion/hydrophobicity properties. The critical value of the geometric parameter group $g^c_{k,n}$ is crucial for the design of surface structure for adhesion and superhydrophobic properties, and patterned surface for cell traction measurement.[23] For example, the fiber size should be in a specific range defined by the lower and upper limits for both strong and robust adhesion,[3] or for stable and robust Cassie state for superhydrophobic dewetting properties.[10] In cell traction measurement, the pillar size and aspect ratio of the patterned substrate should be properly designed in order to achieve a large range of substrate flexibility without causing error by the self-bunching of pillars.[23] Overall, this parameter group should be important for a consistent design of the pillar-like surface in the application of micro- and nanotechnology and cell biology.

This research was supported by the National Natural Science Foundation of China under Grant Nos. 10872115, 11025208, and 11221202 and the State Key Laboratory of Explosive Science and Technology of Beijing Institute of Technology (YBKT12-05).

1Y. Su, B. Ji, Y. Huang, and K. Hwang, J. Mater. Sci. **42**(21), 8885–8893 (2007).
2K. Autumn, Y. A. Liang, S. T. Hsieh, W. Zesch, W. P. Chan, T. W. Kenny, R. Fearing, and R. J. Full, Nature **405**(6787), 681–685 (2000).
3H. Yao and H. Gao, J. Mech. Phys. Solids **54**(6), 1120–1146 (2006).
4H. J. Gao and H. M. Yao, Proc. Natl. Acad. Sci. U.S.A. **101**(21), 7851–7856 (2004).
5E. Arzt, S. Gorb, and R. Spolenak, Proc. Natl. Acad. Sci. U.S.A. **100**(19), 10603–10606 (2003).
6B. N. J. Persson, J. Chem. Phys. **118**(16), 7614–7621 (2003).
7C. Y. Hui, A. Jagota, Y. Y. Lin, and E. J. Kramer, Langmuir **18**(4), 1394–1407 (2002).
8H. Gao, B. Ji, M. J. Buehler, and H. Yao, Mol. Cell. Biomech. **1**(1), 37–52 (2004).
9X. F. Gao and L. Jiang, Nature **432**(7013), 36 (2004).
10Y. Su, B. Ji, K. Zhang, H. Gao, Y. Huang, and K. Hwang, Langmuir **26**(7), 4984–4989 (2010).
11Y. Su, B. Ji, Y. Huang, and K.-c. Hwang, Langmuir **26**(24), 18926–18937 (2010).
12Y. Su, S. He, B. Ji, Y. Huang, and K.-C. Hwang, Appl. Phys. Lett. **99**, 263704 (2011).
13K. Zhang and B. Ji, J. Comput. Theor. Nanosci. **9**(6), 831–836 (2012).
14A. K. Geim, S. V. Dubonos, I. V. Grigorieva, K. S. Novoselov, A. A. Zhukov, and S. Y. Shapoval, Nature Mater. **2**(7), 461–463 (2003).
15N. J. Glassmaker, A. Jagota, C. Y. Hui, and J. Kim, J. R. Soc., Interface **1**(1), 23–33 (2004).
16Y. Su, J. Wu, Z. Fan, K.-C. Hwang, J. Song, Y. Huang, and J. A. Rogers, J. Mech. Phys. Solids **60**(3), 487–508 (2012).
17J. M. Gere and S. P. Timoshenko, *Mechanics of Materials: Solutions Manual* (Nelson Thornes, 2003).
18C. Y. Hui, Y. Y. Lin, J. M. Baney, and A. Jagota, J. Adhes. Sci. Technol. **14**(10), 1297–1319 (2000).
19E. E. Williams and J. A. Peterson, Science **215**(4539), 1509–1511 (1982).
20H. J. Gao, B. H. Ji, I. L. Jager, E. Arzt, and P. Fratzl, Proc. Natl. Acad. Sci. U.S.A. **100**(10), 5597–5600 (2003).
21B. H. Ji and H. J. Gao, J. Mech. Phys. Solids **52**(9), 1963–1990 (2004).
22See supplementary material at http://dx.doi.org/10.1063/1.4762822 for an analysis of the asymmetric deformation in fiber bunching.
23J. Fu, Y.-K. Wang, M. T. Yang, R. A. Desai, X. Yu, Z. Liu, and C. S. Chen, Nat. Methods **7**(9), 733–U795 (2010).

Supplementary material

Why haven't the hairs on the feet of gecko been smaller?

Yewang Su, Shijie He, Keh-Chih Hwang and Baohua Ji

S1. The asymmetric deformation of fiber bunching

For simplicity and clarity of the explanation of this problem, we consider the case of two fibers (i.e., $n=2, m=1$, and the two fibers are identical in terms of the fiber size and mechanical properties). The ideas can be extended to the analysis of multiple fibers.

For the asymmetric deformation of two fibers, without loss of generality, we assume the deflection of the tip of one fiber (denoted as fiber #1) as $w_{k,2}+\delta$, and the angle of the neutral axis at the tip is $\theta(\theta\neq 0)$ (in comparison, for symmetric deformation the deflection and angle are both identical between the two fibers, which are $w_{k,2}$ and $\theta=0$, respectively), and the deflection and angle of the other fiber (denoted as fiber #2) are $w_{k,2}-\delta$ and $-\theta$, respectively, because of the asymmetry. Then, the deformation energy of the system can be derived using the beam theory as follows.

The deformation energy of the fiber #1 is obtained as

$$u_1=\frac{6EI}{l^3}\left(w_{k,2}+\delta\right)^2+\frac{2EI\theta^2}{l}-\frac{6EI}{l^2}\left(w_{k,2}+\delta\right)\theta \qquad \text{(R1)}$$

and that of the fiber #2 is

$$u_2=\frac{6EI}{l^3}\left(w_{k,2}-\delta\right)^2+\frac{2EI\theta^2}{l}+\frac{6EI}{l^2}\left(w_{k,2}-\delta\right)\theta \qquad \text{(R2)}$$

Therefore, the total deformation energy of the system is

$$U_{k,2}^{a} = u_1 + u_2 = \frac{12EI}{l^3}(w_{k,2}^2 + \delta^2) + \frac{4EI\theta^2}{l} - \frac{12EI}{l^2}\theta\delta \tag{R3}$$

On the other hand, according to Eq. (1) in the manuscript, the total deformation energy of the symmetric deformation is

$$U_{k,2}^{s} = 12EIw_{k,2}^2 \big/ L^3 \text{ (for n=2)} \tag{R4}$$

If we compare the deformation energy between the symmetric and the asymmetric bunching, we have

$$U_{k,2}^{a} - U_{k,2}^{s} = \frac{4EI}{l^3}\left[\left(\theta l - \frac{3}{2}\delta\right)^2 + \frac{3}{4}\delta^2\right] > 0 \tag{R5}$$

Therefore, the deformation energy of the asymmetric bunching is always larger than that of the symmetric bunching. The adhesion energy will not change (for small deformation it is only the function of material properties and fiber size) according to Eq. (2) in the manuscript as

$$W_{k,2} = 3\gamma_s \left[\frac{32R^2\gamma_s\left(1-\nu^2\right)}{\pi E}\right]^{\frac{1}{3}} \tag{R6}$$

therefore, the total free energy of the asymmetric deformation is larger than that of the symmetric deformation. The higher the degree of the asymmetry, the more unstable the asymmetric deformation state.